ACS Energy LETTERS

http://pubs.acs.org/journal/aelccp

LETTER

"Wine-Dark Sea" in an Organic Flow Battery: Storing Negative Charge in 2,1,3-Benzothiadiazole Radicals Leads to Improved Cyclability

Wentao Duan,[†,‡,§] Jinhua Huang,[†,∥,§] Jeffrey A. Kowalski,[†,¶] Ilya A. Shkrob,[†,∥] M. Vijayakumar,[†,‡] Eric Walter,[‡] Baofei Pan,[†,∥] Zheng Yang,[†,‡] Jarrod D. Milshtein,[†,¶] Bin Li,[‡] Chen Liao,[†,∥] Zhengcheng Zhang,[†,∥] Wei Wang,[‡] Jun Liu,[†,‡] Jeffery S. Moore,[†,#] Fikile R. Brushett,[†,¶] Lu Zhang,[*,†,∥] and Xiaoliang Wei[*,†,‡]

[†]Joint Center for Energy Storage Research, Argonne, Illinois 60439, United States

[‡]Pacific Northwest National Laboratory, 902 Battelle Boulevard, Richland, Washington 99352, United States

[∥]Argonne National Laboratory, 9700 Cass Avenue, Argonne, Illinois 60439, United States

[¶]Massachusetts Institute of Technology, 77 Massachusetts Avenue, Cambridge, Massachusetts 02139, United States

[#]The Beckman Institute for Advanced Science and Technology and The Department of Chemistry, University of Illinois Urbana−Champaign, 405 North Mathews Avenue, Urbana, Illinois 81801, United States

Supporting Information

ABSTRACT: **Redox-active organic materials (ROMs) have shown great promise for redox flow battery applications but generally encounter limited cycling efficiency and stability at relevant redox material concentrations in nonaqueous systems. Here we report a new heterocyclic organic anolyte molecule, 2,1,3-benzothiadiazole, that has high solubility, a low redox potential, and fast electrochemical kinetics. Coupling it with a benchmark catholyte ROM, the nonaqueous organic flow battery demonstrated significant improvement in cyclable redox material concentrations and cell efficiencies compared to the state-of-the-art nonaqueous systems. Especially, this system produced exceeding cyclability with relatively stable efficiencies and capacities at high ROM concentrations (>0.5 M), which is ascribed to the highly delocalized charge densities in the radical anions of 2,1,3-benzothiadiazole, leading to good chemical stability. This material development represents significant progress toward promising next-generation energy storage.**

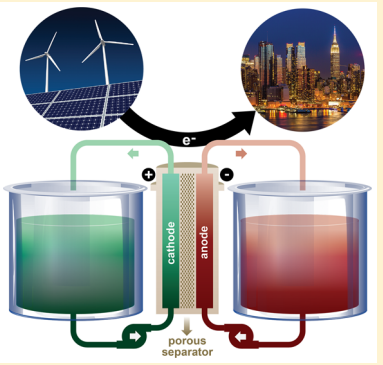

Scalable electrical energy storage will play an important role in the future "smart grid" by improving the output quality of electricity generated from intermittent renewable power sources and increasing the grid asset utilization efficiency. Redox flow batteries are emerging candidates for grid-scale stationary energy storage applications.[1−3] Externally stored electrolyte solutions of redox-active materials circulate through the positive and negative electrode compartments for energy conversion and are denoted as catholyte and anolyte, respectively. The spatial separation between the electrodes and the electrolyte reservoirs decouples the power and energy in flow batteries; the former is related to the electrode area, while the latter depends on the electrolyte volume. Such a feature offers significant advantages over conventional lithium ion batteries and allows customizable designs to meet diverse demands of various energy/power ratios in practical grid applications.[4−6] Flow batteries with aqueous electrolytes are becoming commercially available, but their energy densities are limited by the intrinsically low operating voltages (<1.8 V).[7,8] An attractive alternative to address this limitation is to develop nonaqueous flow batteries, taking advantage of the wider electrochemical windows (>2 V), which offers a new pathway to achieve high energy density and access attractive new redox materials. Nonaqueous redox flow batteries based on inorganic active materials (such as sulfur and iodine species),[9,10] redox-active polymers,[11] and organometallic compounds[12,13] have been developed, as well as hybrid ones such as semisolid[14] and redox-targeting flow batteries,[15] attempting to harvest high energy densities. Besides, redox-active organic materials

Received: March 25, 2017
Accepted: April 24, 2017
Published: April 24, 2017

ACS Publications © XXXX American Chemical Society

DOI: 10.1021/acsenergylett.7b00261
ACS Energy Lett. 2017, 2, 1156−1161

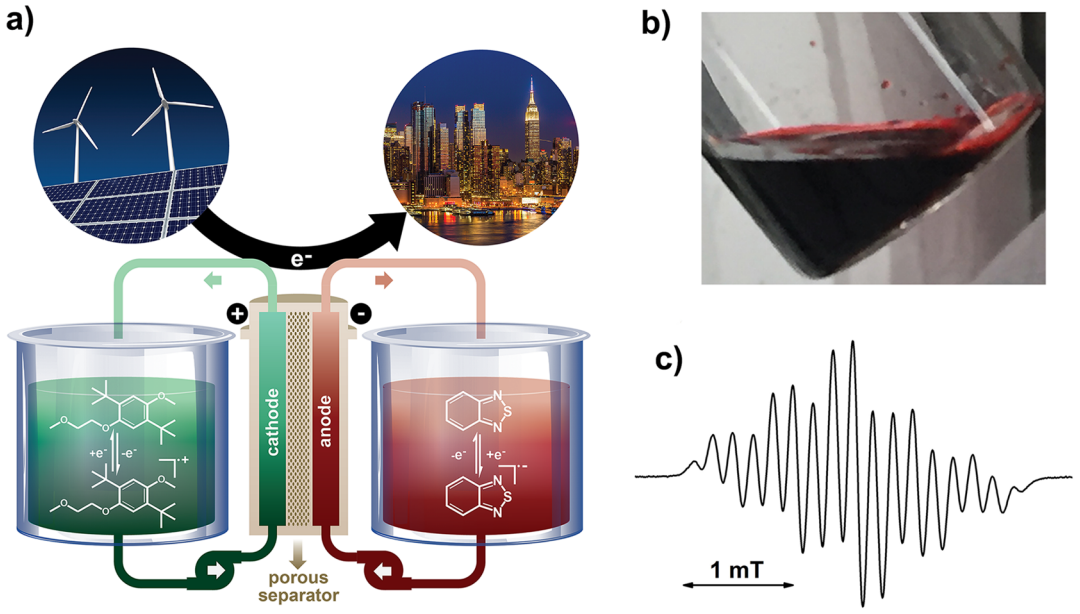

Figure 1. (a) Illustration of the BzNSN/DBMMB flow battery and the cell reactions. (b) Photo of a concentrated, "wine-dark" $BzNSN^{\bullet-}$ electrolyte. (c) EPR spectrum of a dilute $BzNSN^{\bullet-}$ electrolyte.

(ROMs) have drawn particular attention for use in nonaqueous flow batteries, primarily because of their structural diversity, tailorable solubility, environmental benignancy, and potentially low costs.[16−20] Such a combination of favorable properties has also sparked interests in using ROMs for aqueous flow batteries.[21−26]

To realize this promise, nonaqueous flow batteries should be electrochemically evaluated under practically relevant conditions that give them their competitive edge at high ROM concentrations and operational currents and with good figure-of-merit performance delivery including the high efficiency. A recent technoeconomic cost analysis[27] favors ROMs with low equivalent weight (<150 g (mol e^-)$^{-1}$), high molarity (>5 M), sufficiently separated redox potentials (>3 V), and high chemical stability as the keys to approaching the battery cost target of $100 per kWh. Development of such ROMs is extremely challenging; even one of these criteria (of the low equivalent weight) leaves very limited space for molecular design. In reality, the majority of reported nonaqueous flow batteries used limited ROM concentrations (~0.1 M) and/or voltages (<2 V).[28,29] This is mostly because of low ROM solubilities and narrow redox potential gaps between catholyte and anolyte ROMs, as well as the difficulty of operating nonaqueous flow cells in high-concentration regimes. The challenges include increased electrolyte viscosity and high resistance in concentrated electrolytes. The fact that many nonaqueous systems were studied under nonflow conditions reflects these technical obstacles. Another formidable problem stymying the development of nonaqueous flow batteries is the irreversible capacity loss.[30,31] A major cause is the decomposition of charged ROM molecules (in their reactive radical ion forms) that may chemically react with each other, neutral ROM molecules, supporting salts, and solvents.[32] Therefore, development of highly soluble ROMs with suitable redox potentials and high chemical stability is the key to achieving promising cell performance in nonaqueous organic flow batteries.

Here we report a new heterocyclic anolyte material, 2,1,3-benzothiadiazole (BzNSN), for use in nonaqueous flow batteries. Due to its high electron affinity, the BzNSN has been frequently used as an electron acceptor in polymeric solar cells.[33] This BzNSN molecule satisfies several requirements of an anolyte material for flow batteries as it has low equivalent weight, high solubility, and low redox potential; these are three important factors in determining the theoretical energy density and electrolyte cost of a flow battery system. For one-electron reduction, BzNSN exhibits an equivalent weight of 136 g (mol e^-)$^{-1}$, which is well below the threshold value of 150 g (mol e^-)$^{-1}$.[27] BzNSN has a high solubility of 5.7 M in pure acetonitrile (MeCN) (and in other commonly used organic solvents; see Table S1 in the Supporting Information) and of 2.1 M in 2.1 M lithium bis(trifluoromethylsulfonyl)imide (LiTFSI) in MeCN. These values are among the highest solubilities obtained for ROMs in flow battery electrolytes. MeCN is a favored solvent for nonaqueous flow batteries because of low viscosity and high conductivity with dissolved salts that are particularly attractive for battery tests under relevant conditions.[16] More importantly, good cyclability was achieved in a full-cell organic flow battery that couples BzNSN with 2,5-di-*tert*-butyl-1-methoxy-4-[2′-methoxyethoxy]benzene (DBMMB), a liquid catholyte material that is highly miscible with MeCN.[34] The half-cell reactions are illustrated in Figure 1a. When the cell is charged, the colorless BzNSN is reduced at the anolyte side to the "wine-dark" open-shell $BzNSN^{\bullet-}$ radical anion (Figure 1b). The radical nature was demonstrated with electron paramagnetic resonance (EPR) spectroscopy (Figure 1c). The splitting pattern in the EPR spectrum reflects the superhyperfine interactions between the unpaired electron with the multiple protons on the aromatic rings. The radical retention of $BzNSN^{\bullet-}$ in the LiTFSI/MeCN electrolyte as a function of time is illustrated in Figure S1 in the Supporting Information. Meanwhile, the pale yellow DBMMB is oxidized at the catholyte side to the yellowish dark-green $DBMMB^{\bullet+}$ radical cation (Figure S2 in the Supporting Information).

DOI: 10.1021/acsenergylett.7b00261
ACS Energy Lett. 2017, 2, 1156−1161

Cyclic voltammetry (CV) tests were performed to determine redox potentials and identify redox species for BzNSN and DBMMB. Figure 2a displays the CV trace of a mixed-reactant electrolyte containing an equal molarity (0.1 M) of BzNSN and DBMMB in 1 M LiTFSI in MeCN. BzNSN shows well-defined oxidation and reduction peaks with an average redox potential of −1.58 V vs Ag/Ag^+. Such a redox potential is among the lowest reported for anolyte materials in nonaqueous flow batteries. CV results with 5 mM BzNSN suggest electrochemical reversibility of BzNSN reduction. Not only do the positions of these redox peaks stay almost unchanged with the scan rate ranging from 10 to 200 mV s^{-1}, but also all of the peak current ratios are very close to unity (inset of Figure S3a in the Supporting Information). With a redox potential of +0.78 V vs Ag/Ag^+ for DBMMB, this new BzNSN/DBMMB flow battery acquires a theoretical cell potential of 2.36 V. The electron-transfer kinetics of BzNSN and DBMMB were studied using linear sweep voltammetry (LSV) with a glassy carbon rotating disk electrode (RDE). LSV curves exhibit mass-transport-controlled limiting currents in well-defined plateau shapes at rotation rates ranging from 300 to 2100 rpm (Figure 2b). Koutecky−Levich analysis (Figure 2c,d) yields electrochemical rate constants of 0.9×10^{-2} cm s^{-1} for reduction of BzNSN and 1.0×10^{-2} cm s^{-1} for oxidation of DBMMB. These kinetic parameters are on par with, or significantly greater than, other reported redox systems for nonaqueous flow batteries as well as aqueous quinone-like compounds.[21,35] The rapid kinetics of these ROMs is expected to lead to fast electron-transfer processes and high flow cell efficiencies. Due to facilitated mass transfer by flowing electrolytes, diffusivities of these molecules are not as relevant for flow batteries, although they can be obtained from both CV and LSV (Figure S3b,c in the Supporting Information).

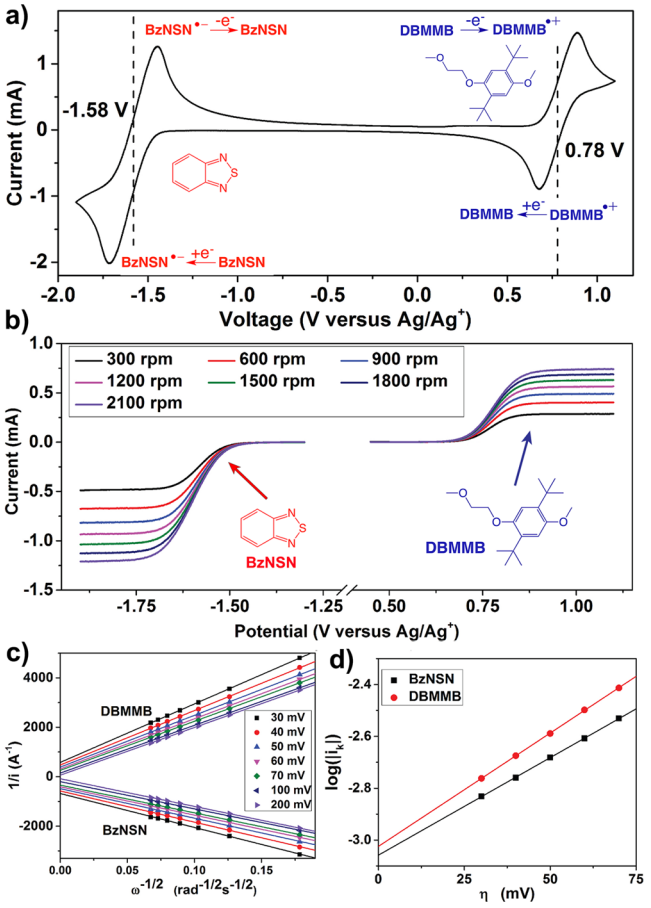

Figure 2. Voltammetry results for BzNSN and DBMMB: (a) CV curve for 0.1 M BzNSN and 0.1 M DBMMB in 1 M LiTFSI/MeCN at a scan rate of 100 mV s^{-1}; (b) LSV curves for 5.0 mM BzNSN and 5.0 mM DBMMB in 1 M LiTFSI/MeCN at a voltage scan rate of 5 mV s^{-1}; (c) linear plots of the current (i) as a function of the square root of the rotation rate (ω) under an overpotential (η) from 30 to 200 mV; (d) dependence of kinetics-controlled current (i_k) on η gives exchange currents (i_0) of 0.87 mA for BzNSN and 0.95 mA for DBMMB by extrapolating η to 0.

Such a redox potential is among the lowest reported for anolyte materials in nonaqueous flow batteries. CV results with 5 mM BzNSN suggest electrochemical reversibility of BzNSN reduction. Not only do the positions of these redox peaks stay almost unchanged with the scan rate ranging from 10 to 200 mV s^{-1}, but also all of the peak current ratios are very close to unity (inset of Figure S3a in the Supporting Information). With a redox potential of +0.78 V vs Ag/Ag^+ for DBMMB, this new BzNSN/DBMMB flow battery acquires a theoretical cell potential of 2.36 V. The electron-transfer kinetics of BzNSN and DBMMB were studied using linear sweep voltammetry (LSV) with a glassy carbon rotating disk electrode (RDE). LSV curves exhibit mass-transport-controlled limiting currents in well-defined plateau shapes at rotation rates ranging from 300 to 2100 rpm (Figure 2b). Koutecky−Levich analysis (Figure 2c,d) yields electrochemical rate constants of 0.9×10^{-2} cm s^{-1} for reduction of BzNSN and 1.0×10^{-2} cm s^{-1} for oxidation of DBMMB. These kinetic parameters are on par with, or significantly greater than, other reported redox systems for nonaqueous flow batteries as well as aqueous quinone-like compounds.[21,35] The rapid kinetics of these ROMs is expected to lead to fast electron-transfer processes and high flow cell efficiencies. Due to facilitated mass transfer by flowing electrolytes, diffusivities of these molecules are not as relevant for flow batteries, although they can be obtained from both CV and LSV (Figure S3b,c in the Supporting Information).

The cycling stability is of critical importance to flow batteries as it determines the lifetime and levelized cost of flow batteries. In certain flow battery systems such as all-vanadium, the capacity loss is caused by unbalanced redox material transfer and can be restored conveniently through electrolyte remixing or hydraulic pressure regulation.[36] However, irreversible capacity loss can also occur if the redox materials are involved in parasitic side reactions resulting in their irreversible decomposition or chemical incompatibility with supporting electrolytes or between redox species. This is especially important for neutral, closed-shell ROMs because their electrochemical reactions generate chemically reactive radical ions. The high stability of BzNSN species in the LiTFSI/MeCN supporting electrolyte was first demonstrated in bulk electrolysis (BE) tests using 10 mM BzNSN (Figure S4a in the Supporting Information). The house-built BE cell (Figure S5a in the Supporting Information) used graphite felt strips as both working and counter electrodes separated by porous fritted glass.[37] Electrochemical charge/discharge cycling was carried

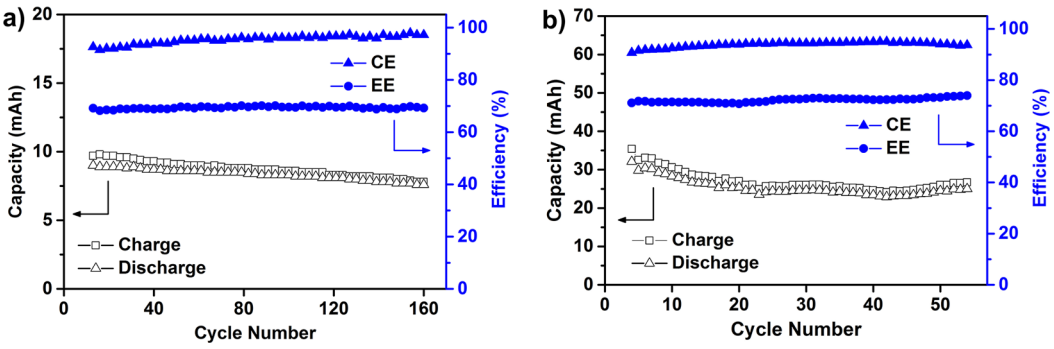

Figure 3. Efficiency and capacity of the BzNSN/DBMMB flow cells using mixed-reactant electrolytes: (a) 0.1 M at 40 mA cm^{-2} with a Celgard 4560 separator; (b) 0.5 M at 10 mA cm^{-2} with a Daramic separator (thickness 800 μm).

DOI: 10.1021/acsenergylett.7b00261
ACS Energy Lett. 2017, 2, 1156−1161

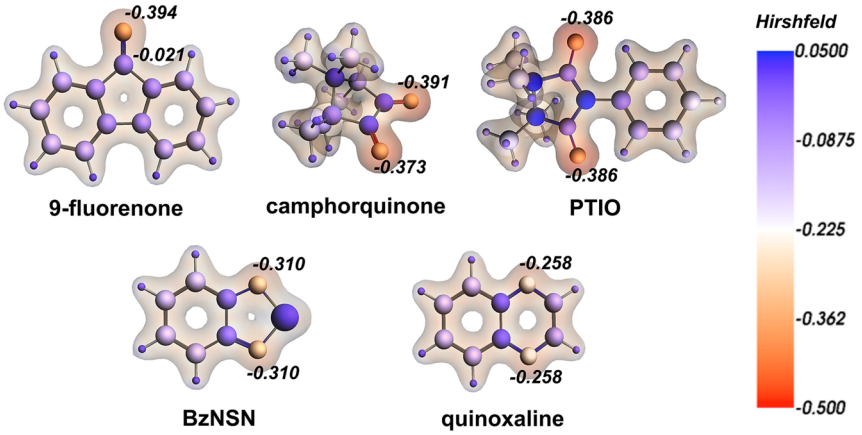

Figure 4. Hirshfeld charge densities at the redox-active sites in reported organic radical anion anolyte molecules.

out at a constant current of 2.68 mA, corresponding to a 1C charge rate, and with 50% of the theoretical capacity accessed. After the initial cycles, a stable columbic efficiency (CE) of ∼90% and constant capacity were maintained throughout the 25 cycles. The near-identical voltage curves along the cycling (Figure S4b in the Supporting Information) suggest clean electrochemistry for BzNSN. These rapid and simple tests indicate that BzNSN would be a viable candidate for flow batteries.

Demonstrating nonaqueous flow batteries under practically relevant conditions is challenging. The lack of high-performance membranes that combine high ionic conductivity and selectivity is one of the major limiting factors for delivering high-current, low-crossover cell performance. Here we used Celgard and Daramic porous separators that have high ionic conductivity yet low selectivity due to the relatively large pore size with respect to molecular size. Mixed-reactant electrolytes with a 1:1 molar ratio of BzNSN and DBMMB were used to decrease redox material crossover.[38,39] Figure 3a shows the cycling efficiency and capacity of the BzNSN/DBMMB flow cell at 0.1 M mixed-reactant electrolytes. The flow cell (Figure S5b in the Supporting Information) using a Celgard 4560 porous separator (laminated polypropylene film thickness 110 μm, base polypropylene film thickness 25 μm, pore size 64 nm, porosity 55%) exhibited an area-specific resistivity (ASR) of ∼1.3 Ω cm^2 (please see the impedance data in Figure S6 in the Supporting Information). Such a low flow cell ASR allows charge/discharge operations under current densities as high as 60 mA cm^{-2} without excessively compromising efficiency and capacity outputs (Figure S7a in the Supporting Information). For example, a material utilization ratio of ∼80% and an energy efficiency (EE) of ∼60% were obtained at 60 mA cm^{-2}, indicative of excellent rate performance achievable for this nonaqueous flow battery. The flow cells exhibited well-defined plateaus in charge/discharge voltage curves at these tested current densities (Figure S7b in the Supporting Information). Galvanostatic cell cycling at 40 mA cm^{-2} generated relatively stable efficiencies over ∼150 cycles with an average CE of 95%, voltaic efficiency (VE) of 73%, EE of 69%, and material utilization of ∼80%. Such a rate performance is comparable to that of neutral electrolyte (e.g., NaCl)-based aqueous flow cells[22,40] and significantly better than that of most nonaqueous flow cells.[41−43]

Increasing the redox materials' concentrations to a more relevant level, for example, 0.5 M, encounters challenging situations for good cycling, such as greatly increased electrolyte viscosity and redox material crossover. This has led to increased cell overpotential and reduced efficiency. To address these limitations, a thicker Daramic porous separator (800 μm thick, median pore size 0.15 μm) was used to reduce redox material crossover, while a lower current density (10 mA cm^{-2}) was used to mitigate cell polarization. As shown in Figure 3b, the 0.5 M flow cell yielded a CE of 94%, VE of 77%, EE of 72%, and material utilization of ∼60% for 50 cycles. The time needed to complete one charge/discharge cycle was 1−1.5 h (Figure S8a in the Supporting Information). The discharge energy density during cycling was around 6−8 Wh L^{-1}. More importantly, both the 0.1 and 0.5 M flow cells demonstrated relatively stable capacities throughout their cycling. The 0.1 M cell shows an average capacity retention of 99.9% per cycle. On the other hand, the capacities of the 0.5 M cell exhibit a gradual drop during the first 20 cycles and then become relatively stable despite a slightly unsteady capacity profile presumably due to temperature fluctuations. The initial capacity drop is ascribed to the increased cell overpotential along the cycling, as indicated by the voltage curves of the 4th and 22nd cycles in Figure S8b in the Supporting Information, although side reactions can be a possibility as well. In addition, even more stable cycling with almost no capacity fading for 40 cycles was obtained in a flow cell containing 0.3 M ROMs in 1,2-dimethoxyethane (DME) (Figure S9 in the Supporting Information) as DME is generally more stable toward organic radical anions.[32,39] So far, the high-concentration cell efficiency and stability are among the best flow cell performance achieved in nonaqueous flow batteries, although further improvement is still needed to make this system practically attractive. These results also demonstrate the good chemical stability of the redox species.

We attribute the good stability of the BzNSN redox species to the high degree of charge delocalization in the BzNSN$^{\bullet-}$. This leads to low charge density at the redox-active N sites, making the locus of the excess electron less vulnerable to chemical attack from the solvent molecules. To demonstrate this point, density functional theory (DFT) calculations were carried out. The Hirshfeld charge density at redox-active sites of BzNSN$^{\bullet-}$ and several previously reported anolyte molecules are shown in Figure 4. The redox-active carbonyl groups in 9-fluorenone[32] and camphorquinone[30] have the highest electron densities. Thus, parasitic reactions involving the carbonyl oxygen (such as protonation or electrophilic attacks on solvent molecules) can be rapid, which may be closely related with the

DOI: 10.1021/acsenergylett.7b00261
ACS Energy Lett. 2017, 2, 1156−1161

fast capacity fading of corresponding flow cells in nitrile or carbonate solvents. The same applies to the nitroxyl group in PTIO.[31] In contrast, the negative charges in BzNSN and quinoxaline are distributed over their conjugated π-bond systems, reducing the excess negative charge in the individual atoms. This accounts for the improved stability of their radical anions in carbonate or nitrile solvents, as demonstrated by their good flow cell cycling stability in these solvents.[28] These examples support the aforementioned general argument, although other more subtle factors may also be important.

Further increase of ROM concentrations to 1.0 M led to even lower cell efficiency due to the increase in electrolyte viscosity and cell polarization (Figure S10 in the Supporting Information). Further improvement of flow cell performance especially at the high-concentration regime indeed requires good understanding of the origin of electrolyte viscosity, circumvention of the side reaction pathways, and optimization of the cell design to facilitate mass and charge transfers.[44] These studies are underway.

To conclude, we have successfully demonstrated BzNSN as a promising anolyte candidate material for nonaqueous organic redox flow batteries. This readily accessible ROM fortuitously combines low equivalent weight (136 g (mol e^-)$^{-1}$), low redox potential (−1.58 V vs Ag/Ag$^+$), high solubility in organic solvents (>5 M), and rapid electrochemical kinetics. Most importantly, it demonstrated relatively stable efficiencies and capacities over extended cycling under tested flow cell conditions, that is, at relevant redox concentrations (0.1 and 0.5 M) and operational currents (up to 60 mA cm^{-2}), in a proof-of-principle 2.36 V nonaqueous organic flow battery. The performance parameters obtained in the BzNSN/DBMMB system greatly exceed the ones observed in other reported systems of this kind. For this reason, we argue that the development of this system is a significant step toward realization of practically feasible nonaqueous flow batteries. Although still compromised by higher electrolyte viscosity at elevated redox concentrations, our results bring to the forefront an important indication that the cell efficiencies can be improved by tuning the test conditions of these flow cells. Thus, more engineering work, such as advanced cell designs and selective membranes, is critically needed in the future to address the current challenges to realize the promise of such organic flow cells.

■ ASSOCIATED CONTENT

Supporting Information

The Supporting Information is available free of charge on the ACS Publications website at DOI: 10.1021/acsenergylett.7b00261.

Experimental procedures, BzNSN solubilities in other solvents, more CV analysis, BE cycling data, and additional cycling data of the 0.1, 0.3 (in DME), 0.5, and 1.0 M flow cells (PDF)

■ AUTHOR INFORMATION

Corresponding Authors

*E-mail: luzhang@anl.gov (L.Z.).
*E-mail: Xiaoliang.Wei@pnnl.gov (X.W.).

ORCID

Ilya A. Shkrob: 0000-0002-8851-8220
Wei Wang: 0000-0002-5453-4695
Jun Liu: 0000-0001-8663-7771
Fikile R. Brushett: 0000-0002-7361-6637
Xiaoliang Wei: 0000-0002-7692-2357

Author Contributions

[§]W.D. and J.H. contribute equally to this paper.

Notes

The authors declare no competing financial interest.

■ ACKNOWLEDGMENTS

The research was financially supported by the Joint Center for Energy Storage Research (JCESR), an Energy Innovation Hub funded by the U.S. Department of Energy, Office of Science, Basic Energy Sciences. EPR measurement was supported by the William R. Wiley Environmental Molecular Sciences Laboratory (EMSL), a national scientific user facility sponsored by DOE's Office of Biological and Environmental Research. PNNL is a multiprogram national laboratory operated by Battelle for DOE under Contract DE-AC05-76RL01830.

■ REFERENCES

(1) Dunn, B.; Kamath, H.; Tarascon, J.-M. Electrical Energy Storage for the Grid: A Battery of Choices. *Science* **2011**, *334*, 928−935.
(2) Yang, Z.; Zhang, J.; Kintner-Meyer, M. C. W.; Lu, X.; Choi, D.; Lemmon, J. P.; Liu, J. Electrochemical Energy Storage for Green Grid. *Chem. Rev.* **2011**, *111*, 3577−3613.
(3) Wang, W.; Luo, Q.; Li, B.; Wei, X.; Li, L.; Yang, Z. Recent Progress in Redox Flow Battery Research and Development. *Adv. Funct. Mater.* **2013**, *23*, 970−986.
(4) Soloveichik, G. L. Flow Batteries: Current Status and Trends. *Chem. Rev.* **2015**, *115*, 11533−58.
(5) Noack, J.; Roznyatovskaya, N.; Herr, T.; Fischer, P. The Chemistry of Redox-Flow Batteries. *Angew. Chem., Int. Ed.* **2015**, *54*, 9776−9809.
(6) Weber, A.; Mench, M.; Meyers, J.; Ross, P.; Gostick, J.; Liu, Q. Redox flow batteries: a review. *J. Appl. Electrochem.* **2011**, *41*, 1137−1164.
(7) Leung, P.; Li, X.; Ponce de Leon, C.; Berlouis, L.; Low, C. T. J.; Walsh, F. C. Progress in redox flow batteries, remaining challenges and their applications in energy storage. *RSC Adv.* **2012**, *2*, 10125−10156.
(8) Skyllas-Kazacos, M.; Chakrabarti, M. H.; Hajimolana, S. A.; Mjalli, F. S.; Saleem, M. Progress in Flow Battery Research and Development. *J. Electrochem. Soc.* **2011**, *158*, R55−R79.
(9) Chen, H.; Lu, Y. A high-energy-density multiple redox semi-solid-liquid flow battery. *Adv. Energy Mater.* **2016**, *6*, 1502183.
(10) Pratt, H. D.; Hudak, N. S.; Fang, X.; Anderson, T. M. A polyoxometalate flow battery. *J. Power Sources* **2013**, *236*, 259−264.
(11) Nagarjuna, G.; Hui, J.; Cheng, K. J.; Lichtenstein, T.; Shen, M.; Moore, J. S.; Rodriguez-Lopez, J. Impact of Redox-Active Polymer Molecular Weight on the Electrochemical Properties and Transport Across Porous Separators in Nonaqueous Solvents. *J. Am. Chem. Soc.* **2014**, *136*, 16309−16316.
(12) Sevov, C. S.; Fisher, S. L.; Thompson, L. T.; Sanford, M. S. Mechanism-Based Development of a Low-Potential, Soluble, and Cyclable Multielectron Anolyte for Nonaqueous Redox Flow Batteries. *J. Am. Chem. Soc.* **2016**, *138*, 15378−15384.
(13) Ding, Y.; Zhao, Y.; Li, Y.; Goodenough, J. B.; Yu, G. A high-performance all-metallocene-based, non-aqueous redox flow battery. *Energy Environ. Sci.* **2017**, *10*, 491−497.
(14) Duduta, M.; Ho, B.; Wood, V. C.; Limthongkul, P.; Brunini, V. E.; Carter, W. C.; Chiang, Y. M. Semi-Solid Lithium Rechargeable Flow Battery. *Adv. Energy Mater.* **2011**, *1*, 511−516.
(15) Jia, C.; Pan, F.; Zhu, Y.; Huang, Q.; Lu, L.; Wang, Q. High−energy density nonaqueous all redox flow lithium battery enabled with a polymeric membrane. *Sci. Adv.* **2015**, *1*, e1500886.
(16) Gong, K.; Fang, Q.; Gu, S.; Li, S. F. Y.; Yan, Y. Nonaqueous redox-flow batteries: organic solvents, supporting electrolytes, and redox pairs. *Energy Environ. Sci.* **2015**, *8*, 3515−3530.

DOI: 10.1021/acsenergylett.7b00261
ACS Energy Lett. 2017, 2, 1156−1161

(17) Winsberg, J.; Hagemann, T.; Janoschka, T.; Hager, M. D.; Schubert, U. S. Redox-Flow Batteries: From Metals to Organic Redox-Active Materials. *Angew. Chem., Int. Ed.* **2017**, *56*, 686−711.
(18) Park, M.; Ryu, J.; Wang, W.; Cho, J. Material design and engineering of next-generation flow-battery technologies. *Nat. Rev. Mater.* **2016**, *2*, 16080.
(19) Ding, Y.; Yu, G. A. Bio-inspired, heavy-metal-free, dual-electrolyte liquid battery towards sustainable energy storage. *Angew. Chem., Int. Ed.* **2016**, *55*, 4772−4776.
(20) Zhao, Y.; Ding, Y.; Li, Y.; Peng, L.; Byon, H. R.; Goodenough, J. B.; Yu, G. A chemistry and material perspective on lithium redox flow batteries towards high-density electrical energy storage. *Chem. Soc. Rev.* **2015**, *44*, 7968−7996.
(21) Huskinson, B.; Marshak, M. P.; Suh, C.; Er, S.; Gerhardt, M. R.; Galvin, C. J.; Chen, X.; Aspuru-Guzik, A.; Gordon, R. G.; Aziz, M. J. A metal-free organic-inorganic aqueous flow battery. *Nature* **2014**, *505*, 195−198.
(22) Janoschka, T.; Martin, N.; Martin, U.; Friebe, C.; Morgenstern, S.; Hiller, H.; Hager, M. D.; Schubert, U. S. An aqueous, polymer-based redox-flow battery using non-corrosive, safe, and low-cost materials. *Nature* **2015**, *527*, 78−81.
(23) Liu, T.; Wei, X.; Nie, Z.; Sprenkle, V.; Wang, W. A Total Organic Aqueous Redox Flow Battery Employing a Low Cost and Sustainable Methyl Viologen Anolyte and 4-HO-TEMPO Catholyte. *Adv. Energy Mater.* **2016**, *6*, 1501449.
(24) Winsberg, J.; Stolze, C.; Schwenke, A.; Muench, S.; Hager, M. D.; Schubert, U. S. Aqueous 2,2,6,6-Tetramethylpiperidine-N-oxyl Catholytes for a High-Capacity and High Current Density Oxygen-Insensitive Hybrid-Flow Battery. *ACS Energy Lett.* **2017**, *2*, 411−416.
(25) Janoschka, T.; Martin, N.; Hager, M. D.; Schubert, U. S. An Aqueous Redox-Flow Battery with High Capacity and Power: The TEMPTMA/MV System. *Angew. Chem., Int. Ed.* **2016**, *55*, 14427−14430.
(26) Carretero-Gonzalez, J.; Castillo-Martinez, E.; Armand, M. Highly water-soluble three-redox state organic dyes as bifunctional analytes. *Energy Environ. Sci.* **2016**, *9*, 3521−3530.
(27) Darling, R. M.; Gallagher, K. G.; Kowalski, J. A.; Ha, S.; Brushett, F. R. Pathways to low-cost electrochemical energy storage: a comparison of aqueous and nonaqueous flow batteries. *Energy Environ. Sci.* **2014**, *7*, 3459−3477.
(28) Brushett, F. R.; Vaughey, J. T.; Jansen, A. N. An All-Organic Non-aqueous Lithium-Ion Redox Flow Battery. *Adv. Energy Mater.* **2012**, *2*, 1390−1396.
(29) Sevov, C. S.; Brooner, R. E. M.; Chenard, E.; Assary, R. S.; Moore, J. S.; Rodriguez-Lopez, J.; Sanford, M. S. Evolutionary Design of Low Molecular Weight Organic Anolyte Materials for Applications in Nonaqueous Redox Flow Batteries. *J. Am. Chem. Soc.* **2015**, *137*, 14465−14472.
(30) Park, S. K.; Shim, J.; Yang, J.; Shin, K. H.; Jin, C. S.; Lee, B. S.; Lee, Y. S.; Jeon, J. D. Electrochemical properties of a non-aqueous redox battery with all-organic redox couples. *Electrochem. Commun.* **2015**, *59*, 68−71.
(31) Duan, W.; Vemuri, R. S.; Milshtein, J. D.; Laramie, S.; Dmello, R. D.; Huang, J.; Zhang, L.; Hu, D.; Vijayakumar, M.; Wang, W.; et al. A symmetric organic-based nonaqueous redox flow battery and its state of charge diagnostics by FTIR. *J. Mater. Chem. A* **2016**, *4*, 5448−5456.
(32) Wei, X.; Xu, W.; Huang, J.; Zhang, L.; Walter, E.; Lawrence, C.; Vijayakumar, M.; Henderson, W. A.; Liu, T.; Cosimbescu, L.; et al. Radical Compatibility with Nonaqueous Electrolytes and Its Impact on an All-Organic Redox Flow Battery. *Angew. Chem., Int. Ed.* **2015**, *54*, 8684−8687.
(33) Cheng, P.; Zhan, X. Stability of organic solar cells: challenges and strategies. *Chem. Soc. Rev.* **2016**, *45*, 2544−2582.
(34) Huang, J.; Cheng, L.; Assary, R. S.; Wang, P.; Xue, Z.; Burrell, A. K.; Curtiss, L. A.; Zhang, L. Liquid Catholyte Molecules for Nonaqueous Redox Flow Batteries. *Adv. Energy Mater.* **2015**, *5*, 1401782.
(35) Hagemann, T.; Winsberg, J.; Wild, A.; Schubert, U. S. Synthesis and Electrochemical Study of a TCAA Derivative − A potential bipolar redox-active material. *Electrochim. Acta* **2017**, *228*, 494−502.
(36) Wei, X.; Li, B.; Wang, W. Porous Polymeric Composite Separators for Redox Flow Batteries. *Polym. Rev.* **2015**, *55*, 247−272.
(37) Laramie, S. M.; Milshtein, J. D.; Breault, T. M.; Brushett, F. R.; Thompson, L. T. Performance and cost characteristics of multi-electron transfer, common ion exchange non-aqueous redox flow batteries. *J. Power Sources* **2016**, *327*, 681−692.
(38) Lopezatalaya, M.; Codina, G.; Perez, J. R.; Vazquez, J. L.; Aldaz, A. Optimization Studies on a Fe/Cr Redox Flow Battery. *J. Power Sources* **1992**, *39*, 147−154.
(39) Wei, X.; Duan, W.; Huang, J.; Zhang, L.; Li, B.; Reed, D.; Xu, W.; Sprenkle, V.; Wang, W. A High-Current, Stable Nonaqueous Organic Redox Flow Battery. *ACS Energy Lett.* **2016**, *1*, 705−711.
(40) Zhang, L.; Lai, Q.; Zhang, J.; Zhang, H. A High-Energy-Density Redox Flow Battery based on Zinc/Polyhalide Chemistry. *ChemSusChem* **2012**, *5*, 867−869.
(41) Cappillino, P. J.; Pratt, H. D.; Hudak, N. S.; Tomson, N. C.; Anderson, T. M.; Anstey, M. R. Application of Redox Non-Innocent Ligands to Non-Aqueous Flow Battery Electrolytes. *Adv. Energy Mater.* **2014**, *4*, 1300566.
(42) Kim, H. S.; Yoon, T.; Jang, J.; Mun, J.; Park, H.; Ryu, J. H.; Oh, S. M. A tetradentate Ni(II) complex cation as a single redox couple for non-aqueous flow batteries. *J. Power Sources* **2015**, *283*, 300−304.
(43) Saraidaridis, J. D.; Bartlett, B. M.; Monroe, C. W. Spectroelectrochemistry of Vanadium Acetylacetonate and Chromium Acetylacetonate for Symmetric Nonaqueous Flow Batteries. *J. Electrochem. Soc.* **2016**, *163*, A1239−A1246.
(44) Milshtein, J. D.; Kaur, A. P.; Casselman, M. D.; Kowalski, J. A.; Modekrutti, S.; Zhang, P.; Harsha Attanayake, N.; Elliott, C. F.; Parkin, S. R.; Risko, C.; et al. High current density, long duration cycling of soluble organic active species for non-aqueous redox flow batteries. *Energy Environ. Sci.* **2016**, *9*, 3531−3543.

DOI: 10.1021/acsenergylett.7b00261
ACS Energy Lett. 2017, 2, 1156−1161